

ImageBrush: Learning Visual In-Context Instructions for Exemplar-Based Image Manipulation

Yasheng Sun*

Tokyo Institute of Technology
sun.y.aj@m.titech.ac.jp

Yifan Yang*

Microsoft
yifanyang@microsoft.com

Houwen Peng

Microsoft
houwen.peng@microsoft.com

Yifei Shen

Microsoft
yifeishen@microsoft.com

Yuqing Yang

Microsoft
yuqing.yang@microsoft.com

Han Hu

Microsoft
hanhu@microsoft.com

Lili Qiu[†]

Microsoft
liliqiu@microsoft.com

Hideki Koike

Tokyo Institute of Technology
koike@c.titech.ac.jp

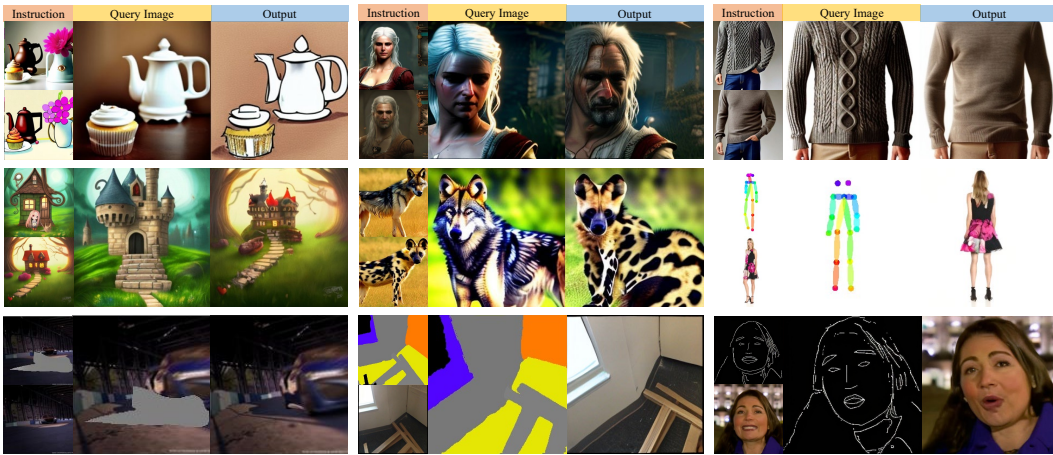


Figure 1: Demo results of the proposed **ImageBrush** framework on various image manipulation tasks. By providing a pair of *task-specific examples* and a *new query image* that share a similar context, ImageBrush accurately *identifies the underlying task* and generates the desired output.

Abstract

While language-guided image manipulation has made remarkable progress, the challenge of how to instruct the manipulation process faithfully reflecting human intentions persists. An accurate and comprehensive description of a manipulation task using natural language is laborious and sometimes even impossible, primarily due to the inherent uncertainty and ambiguity present in linguistic expressions. Is it feasible to accomplish image manipulation without resorting to external cross-modal language information? If this possibility exists, the inherent modality gap would be effortlessly eliminated. In this paper, we propose a novel manipulation methodology, dubbed *ImageBrush*, that learns visual instructions for more accurate image editing. Our key idea is to employ a *pair of transformation images* as *visual instructions*, which not only precisely captures human intention but also facilitates accessibility in real-world scenarios. Capturing visual instructions is particularly challenging because it involves extracting the underlying intentions solely from visual demonstrations and then applying this operation to a new image. To address

*Equal contribution

[†]Corresponding Author

this challenge, we formulate visual instruction learning as a diffusion-based inpainting problem, where the contextual information is fully exploited through an iterative process of generation. A visual prompting encoder is carefully devised to enhance the model’s capacity in uncovering human intent behind the visual instructions. Extensive experiments show that our method generates engaging manipulation results conforming to the transformations entailed in demonstrations. Moreover, our model exhibits robust generalization capabilities on various downstream tasks such as pose transfer, image translation and video inpainting.

1 Introduction

Image manipulation has experienced a remarkable transformation in recent years [49, 14, 36, 71, 21, 29]. The pursuit of instructing manipulation process to align with human intent has garnered significant attention. Language, as a fundamental element of human communication, is extensively studied to guide the manipulation towards intended direction [16, 35, 6, 57, 33, 60, 5]. Despite the universal nature of language-based instructions, there are cases where they fall short in expressing certain world concepts. This limitation necessitates additional efforts and experience in magic prompt engineering, as highlighted in [64]. To compensate linguistic ambiguity, some studies [65, 32, 66] attempt to introduce visual guidance to the manipulation process. However, these approaches heavily rely on cross-modal alignment, which may not always be perfectly matched, thereby resulting in limited adaptability to user instructions.

Is it conceivable to accomplish image manipulation exclusively through visual instructions? If such a capability were attainable, it would not only mitigate the aforementioned cross-modality disparity but also introduce a novel form of interaction for image manipulation. Taking inspiration from the exceptional in-context capabilities by large language models [38, 41, 7] like ChatGPT and GPT-4, we propose to conceptualize the image manipulation task as a visual prompting process. This approach utilizes paired examples to establish visual context, while employing the target image as a query. Recent works [63, 4] reveal the visual in-context ability through a simple Mask Image Modeling [15] scheme. But these researches focus on understanding tasks such as detection and segmentation while only very limited context tasks are studied. Therefore, the in-context potential for image manipulation, where numerous editing choices are involved, is still a promising avenue for exploration.

In contrast to language, which primarily communicates abstract concepts, exemplar-based visual instruction explicitly concretizes manipulation operations within the visual domain. In this way, the network could directly leverage their textures, which eases the hallucination difficulty for some inexpressible concepts (*e.g.*, artist style or convoluted object appearance). On the other hand, the pairwise cases directly exhibit transformation relationship from the visual perspective, thereby facilitating better semantic correspondence learning.

In this paper, we propose an *Exemplar-Based Image Manipulation* framework, **ImageBrush**, which achieves adaptive image manipulation under the instruction of a pair of exemplar demonstrations. Specifically, *no external information from another modality* is needed in our work. The key is to devise *a generative model that tackles both pairwise visual instruction understanding and image synthesis* in a unified manner. To establish the intra-correlations among exemplar transformations and their inter-correlation with the query image, we utilize a grid-like image as model input that concatenates a manipulation example and a target query as [4, 63, 17]. The in-context image manipulation is accomplished by inpainting the lower-right picture. Unlike their approaches forwarding once for final result, we adopt the diffusion process to iteratively enhance in-context learning and refine the synthesized image. This practice not only provide stable training objectives [32], but also mimics the behavior of a painter [9] who progressively fills and tweaks the details.

Although the aforementioned formulation is capable of handling correlation modeling and image generation in a single stroke, it places a significant computational burden on the network, due to the intricate concepts and processes involved. To address this challenge, we delicately design a visual prompting encoder that maximizes the utilization of contextual information, thereby alleviating the complexity of learning. Specifically, **1)** we extract the features of each image and further process them through a transformer module for effective feature exchanging and integration. The obtained features are then injected to a diffusion network with cross-attention to augment its understanding capability. **2)** Inspired by recent advances of visual prompting [52, 73], we design a bounding box incorporation module to take user interactivity into consideration. Different from prior research [52]

which focused on exploring the influence of visual prompt on reasoning ability, our study attempts to utilize it to improve generation conformity by better comprehending the human intent.

Our main contributions can be summarized as follows: **1)** We introduce a novel image manipulation protocol that enables the accomplishment of numerous operations through an in-context approach. Moreover, we developed a metric to assess the quality of the manipulations performed. **2)** We delicately devise a diffusion-based generative framework coupled with a hybrid context injection strategy to facilitate better correlation reasoning. **3)** Extensive experiments demonstrate our approach generates compelling manipulation results aligned with human intent and exhibits robust generalization abilities on various downstream tasks, paving the way for future vision foundation models.

2 Related Work

Language-Guided Image Manipulation. The domain of generating images from textual input [46, 48, 51] has experienced extraordinary advancements, primarily driven by the powerful architecture of diffusion models [19, 48, 53, 54]. Given rich generative priors in text-guided models, numerous studies [33, 11, 37, 2, 2] have proposed their adaptation for image manipulation tasks. To guide the editing process towards the intended direction, researchers have employed CLIP [45] to fine-tune diffusion models. Although these methods demonstrate impressive performance, they often require expensive fine-tuning procedures [24, 58, 25, 5]. Recent approaches [16, 35] have introduced cross-attention injection techniques to facilitate the editing of desired semantic regions on spatial feature maps. Subsequent works further improved upon this technique by incorporating semantic loss [28] or constraining the plugged feature with attention loss [57].

Image Translation. Image translation aims to convert an image from one domain to another while preserving domain-irrelevant characteristics. Early studies [67, 30, 23, 62, 39] have employed conditional Generative Adversarial Networks (GANs) to ensure that the translated outputs conform to the distribution of the target domain. However, these approaches typically requires training a specific network for each translation task and relies on collections of instance images from both the source and target domains. Other approaches [1, 47, 55, 56, 59] have explored exploiting domain knowledge from pre-trained GANs or leveraging augmentation techniques with a single image to achieve image translation with limited data. Another slew of studies [70, 3, 61, 43, 22] focus on exemplar-based image translation due to their flexibility and superior image quality. While the majority of these approaches learn style transfer from a reference image, CoCosNet [72] proposes capturing fine structures from the exemplar image through dense correspondence learning.

3 Method

In this section, we will discuss the details of our proposed *Exemplar-Based Image Manipulation Framework*, **ImageBrush**. The primary objective of this framework is to develop a model capable of performing various image editing tasks by interpreting visual prompts as instructions. To achieve this, the model must possess the ability to comprehend the underlying human intent from contextual visual instructions and apply the desired operations to a new image. The entire pipeline is depicted in Fig. 2, where we employ a diffusion-based inpainting strategy to facilitate unified context learning and image synthesis. To further augment the model’s reasoning capabilities, we meticulously design a visual prompt encoding module aimed at deciphering the human intent underlying the visual instruction.

3.1 Exemplar-Based Image Manipulation

Problem Formulation. Given a pair of manipulated examples $\{\mathbf{E}, \mathbf{E}'\}$ and a query image \mathbf{I} , our training objective is to generate an edited image \mathbf{I}' that adheres to the underlying instructions provided by the examples. Accomplishing this objective necessitates a comprehensive understanding of the intra-relationships between the examples as well as their inter-correlations with the new image. Unlike text, images are not inherently sequential and contain a multitude of semantic information dispersed across their spatial dimensions.

Therefore, we propose a solution in the form of "Progressive In-Painting". A common approach is to utilize cross-attention to incorporate the demonstration examples $\{\mathbf{E}, \mathbf{E}'\}$ and query image \mathbf{I} as general context like previous work [66]. However, we observed that capturing detailed information among visual instructions with cross-attention injection is challenging. To overcome this, we propose learning their low-level context using a self-attention mechanism. Specifically, we concatenate a

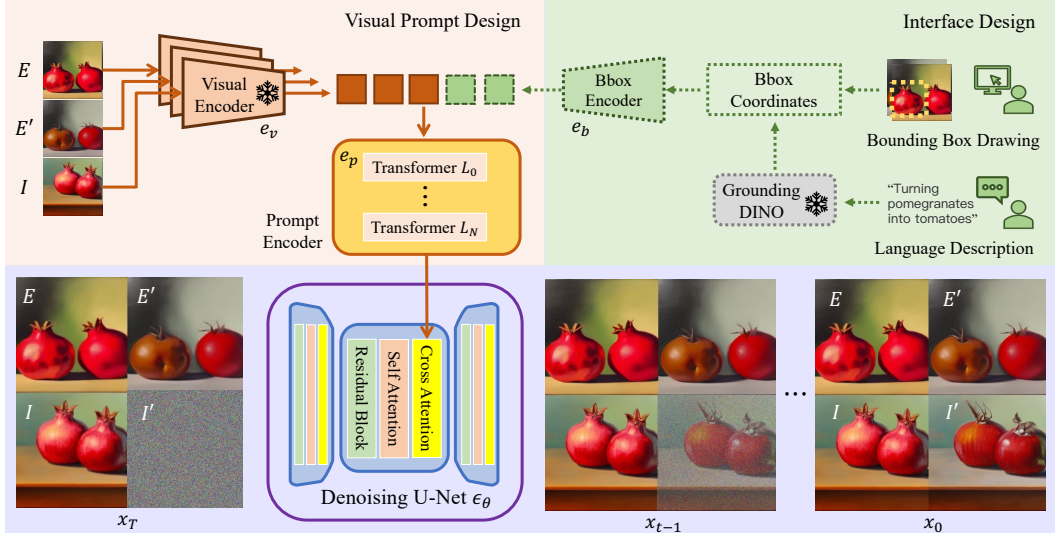


Figure 2: **Illustration of ImageBrush.** We introduce a novel and intuitive way of interacting with images. Users can easily manipulate images by providing a *pair of examples and a query image as prompts* to our system. If users wish to convey more precise instructions, they have the option to inform the model about their areas of interest through manual bounding box annotations or by using language to automatically generate them.

blank image M to the visual instructions and compose a grid-like image $\{\mathbf{E}, \mathbf{E}', \mathbf{I}, M\}$ as illustrated in Fig. 2. The objective is to iteratively recover $\{\mathbf{E}, \mathbf{E}', \mathbf{I}, \mathbf{I}'\}$ from this grid-like image.

Preliminary on Diffusion Model. After an extensive examination of recent generative models, we have determined that the diffusion model [48] aligns with our requirements. This model stands out due to its stable training objective and exceptional ability to generate high-quality images. It operates by iteratively denoising Gaussian noise to produce the image x_0 . Typically, the diffusion model assumes a Markov process [44] wherein Gaussian noises are gradually added to a clean image x_0 based on the following equation:

$$x_t = \sqrt{\alpha_t}x_0 + \sqrt{1 - \alpha_t}\epsilon, \quad (1)$$

where $\epsilon \sim \mathcal{N}(0, \mathbf{I})$ represents the additive Gaussian noise, t denotes the time step and α_t is scalar functions of t . Our training objective is to devise a neural network $\epsilon_\theta(x_t, t, c)$ to predict the added noise ϵ . Empirically, a simple mean-squared error is leveraged as the loss function:

$$L_{simple} := \mathbb{E}_{\epsilon \sim \mathcal{N}(0, \mathbf{I}), x_0, c} \left[\|\epsilon - \epsilon_\theta(x_t, c)\|_2^2 \right], \quad (2)$$

where θ represents the learnable parameters of our diffusion model, and c denotes the conditional input to the model, which can take the form of another image [50], a class label [20], or text [25]. By incorporating this condition, the classifier-free guidance [46] adjusts the original predicted noise $\epsilon_\theta(x_t, \emptyset)$ towards the guidance signal $\epsilon_\theta(x_t, c)$, formulated as

$$\hat{\epsilon}_\theta(x_t, c) = \epsilon_\theta(x_t, \emptyset) + w(\epsilon_\theta(x_t, c) - \epsilon_\theta(x_t, \emptyset)). \quad (3)$$

The w is the guidance scale, determining the degree to which the denoised image aligns with the provided condition c .

Context Learning by Progressive Denoising. The overall generation process is visualized in Fig. 2. Given the denoised result $x_{t-1} = \text{Grid}(\{\mathbf{E}, \mathbf{E}', \mathbf{I}, \mathbf{I}'\}_{t-1})$ from the previous time step t , our objective is to refine this grid-like image based on the contextual description provided in the visual instructions. Rather than directly operating in the pixel space, our model diffuses in the latent space of a pre-trained variational autoencoder, following a similar protocol to Latent Diffusion Models (LDM)[48]. This design choice reduces the computational resources required during inference and enhances the quality of image generation. Specifically, for an image x_t , the diffusion process removes the added Gaussian noise from its encoded latent input $z_t = \mathcal{E}(x_t)$. At the end of the diffusion process, the latent variable z_0 is decoded to obtain the final generated image $x_0 = \mathcal{D}(z_0)$. The encoder \mathcal{E} and decoder \mathcal{D} are adapted from Autoencoder-KL [48], and their weights are fixed in our implementation.

Unlike previous studies that rely on external semantic information [29, 6], here we focus on establishing spatial correspondence within image channels. We introduce a UNet-like network architecture, prominently composed of self-attention blocks, as illustrated in Fig. 2. This design enables our model to attentively process features within each channel and effectively capture their interdependencies.

3.2 Prompt Design for Visual In-Context Instruction Learning

However, relying only on universal correspondence modeling along the spatial channel may not be sufficient for comprehending abstract and complex concepts, which often require reassembling features from various aspects at multiple levels. To address this issue, we propose an additional prompt learning module to enable the model to capture high-level semantics without compromising the synthesis process of the major UNet architecture.

Contextual Exploitation of Visual Prompt. Given the visual prompt $vp = \{\mathbf{E}, \mathbf{E}', \mathbf{I}\}$, we aim to exploit their high-level semantic relationships. To achieve this, a visual prompt module comprising two components is carefully devised, which entails a shared visual encoder e_v and a prompt encoder e_p as illustrated in Fig. 2. For an arbitrary image $\mathbf{I} \in \mathbb{R}^{H \times W \times 3}$ within the visual prompt, we extract its tokenized feature representation f_{img} using the Visual Transformer (ViT)-based backbone e_v . These tokenized features are then fed into the bi-directional transformer e_p , which effectively exploits the contextual information. The resulting feature representation f_c encapsulates the high-level semantic changes and correlations among the examples.

Using the visual prompt, we can integrate high-level semantic information into the UNet architecture by employing the classifier-free guidance strategy as discussed in Section 3.1. This is achieved by injecting the contextual feature into specific layers of the main network through cross-attention.

$$\phi^{l-1} = \phi^{l-1} + \text{Conv}(\phi^{l-1}) \quad (4)$$

$$\phi^{l-1} = \phi^{l-1} + \text{SelfAttn}(\phi^{l-1}) \quad (5)$$

$$\phi^l = \phi^{l-1} + \text{CrossAttn}(f_c) \quad (6)$$

where ϕ^l denotes the input feature of the l -th block, and f_c represents the context feature. Specifically, we select the middle blocks of the UNet architecture, as these blocks have been shown in recent studies to be responsible for processing high-level semantic information [60].

Interface Design for Region of User Interest. Recent advancements in visual instruction systems have demonstrated impressive interactivity by incorporating human prompts [27]. For example, a simple annotation like a red circle on an image can redirect the attention of a pre-trained visual-language model to a specific region [52]. To enhance our model’s ability to capture human intent, we propose the inclusion of an interface that allows individuals to emphasize their focal points. This interface will enable our model to better understand and interpret human intent, leading to more effective comprehension of instructions.

To allow users to specify their area of interest in the examples $\{\mathbf{E}, \mathbf{E}'\}$, we provide the flexibility of using bounding boxes. We found that directly drawing rectangles on the example image led to difficulties in the network’s understanding of the intention. As a result, we decided to directly inject a bounding box into the architecture. For each bounding box $B^i = [\alpha_{min}^i, \beta_{min}^i, \alpha_{max}^i, \beta_{max}^i]$ where $\alpha_{min}^i, \beta_{min}^i$ are the coordinates of the top-left corner and $\alpha_{max}^i, \beta_{max}^i$ are the coordinates of the bottom-right corner, we encode it into a token representation using a bounding box encoder e_b . Formally, this can be expressed as follows:

$$f_b^i = e_b(\text{Fourier}(B^i)) \quad (7)$$

where Fourier is the Fourier embedding [34]. Each bounding box feature is stacked together as f_b , and combined with the previous tokenized image features f_{img} to form $f_g = [f_{img}; f_b]$. This grounded image feature is then passed through e_p for enhanced contextual exploitation. In cases where a user does not specify a bounding box, we employ a default bounding box that covers the entire image.

To simulate user input of region of interest, which can be laborious to annotate with bounding boxes, we use an automatic tool, GroundingDINO [31], to label the focused region based on textual instruction. This approach not only reduces the burden of manual labeling but also provides users with the flexibility to opt for an automatic tool that leverages language descriptions to enhance their intentions, in cases where they are unwilling to draw a bounding box. During the training process, we randomly remove a portion of the bounding boxes to ensure that our model takes full advantage of the visual in-context instructions.

Table 1: **Quantitative Comparison on In-the-wild Dataset.**

Dataset	Exemplar-Based Image Translation			Pose Transfer	Inpainting
	Scannet[12]	LRW(Edge)[10]	LRW(Mask)[10]	UBC-Fashion[69]	DAVIS[42]
TSAM[74]	-	-	-	-	86.84
CoCosNet[72]	19.49	15.44	14.25	38.61	-
ImageBrush	9.18	9.67	8.95	12.99	18.70

¹ We report the widely used FID [18] value here.

4 Experiments

4.1 Experimental Settings

Datasets. Our work leverages four widely used in-the-wild video datasets - Scannet [12], LRW [10], UBCFashion [69], and DAVIS [42] - as well as a synthetic dataset that involves numerous image editing operations. The **Scannet** [12] dataset is a large-scale collection of indoor scenes covering various indoor environments, such as apartments, offices, and hotels. It comprises over 1,500 scenes with rich annotations, of which 1,201 scenes lie in training split, 312 scenes are in the validation set. No overlapping physical location has been seen during training. The **LRW** [10] dataset is designed for lip reading, containing over 1000 utterances of 500 different words with a duration of 1-second video. We adopt 80 percent of their test videos for training and 20 percent for evaluation. The **UBC-Fashion** [69] dataset comprises 600 videos covering a diverse range of clothing categories. This dataset includes 500 videos in the training set and 100 videos in the testing set. No same individuals has been seen during training. The **DAVIS** [42] (Densely Annotated Video Segmentation) dataset is a popular benchmark dataset for video object segmentation tasks. It comprises a total of 150 videos, of which 90 are densely annotated for training and 60 for validation. Similar to previous works [74], we trained our network on the 60 videos in the validation set and evaluate its performance on the original 90 training videos. The synthetic image manipulation dataset is created using image captions of **LAION Improved Aesthetics 6.5+** through Stable Diffusion by [6]. It comprises over 310k editing instructions, each with its corresponding editing pairs. Out of these editing instructions, 260k have more than two editing pairs. We conduct experiment on this set, reserving 10k operations for model validation.

Implementation Details. In our approach, all input images have a size of 256×256 pixels and are concatenated to a 512×512 image as input to the UNet architecture. The UNet architecture, adapted from Stable Diffusion, consists of 32 blocks, where the cross-attention of both upper and lower blocks is replaced with self-attention. We use cross-attention to incorporate the features of the visual prompt module into its two middle blocks. The visual prompt’s shared backbone, denoted as e_v , follows the architecture of EVA-02 [13]. The prompt encoder e_p comprises five layers and has a latent dimension of 768. For the bounding box encoder, denoted as e_b , we adopt a simple MLP following [29]. During training, we set the classifier-free scale for the encoded instruction to 7.5 and the dropout ratio to 0.05. Our implementation utilizes PyTorch [40] and is trained on 24 Tesla V100-32G GPUs for 14K iterations using the AdamW [26] optimizer. The learning rate is set to $1e-6$, and the batch size is set to 288.

Comparison Methods. To thoroughly evaluate the effectiveness of our approach, we compare it against other state-of-art models tailored for specific tasks, including: **SDEdit** [33], a widely-used stochastic differential equation (SDE)-based image editing method; **Instruct-Pix2pix** [6], a cutting-edge language-instructed image manipulation method; **CoCosNet** [72], an approach that employs a carefully designed correspondence learning architecture to achieve exemplar-based image translation; and **TSAM** [74], a model that incorporates a feature alignment module for video inpainting.

4.2 Quantitative Evaluation

Evaluation Metrics. In the image manipulation task, it is crucial for the edited image to align with the intended direction while preserving the instruction-invariant elements in their original form. To assess the degree of agreement between the edited image and the provided instructions, we utilize a cosine similarity metric referred to as **CLIP Direction Similarity** in the CLIP space. In order to measure the level of consistency with original image, we utilize the cosine similarity of the CLIP image embedding, **CLIP Image Similarity**, following the protocol presented in [6]. Additionally, for other generation tasks such as exemplar-based image translation, pose transfer, and video in-painting,

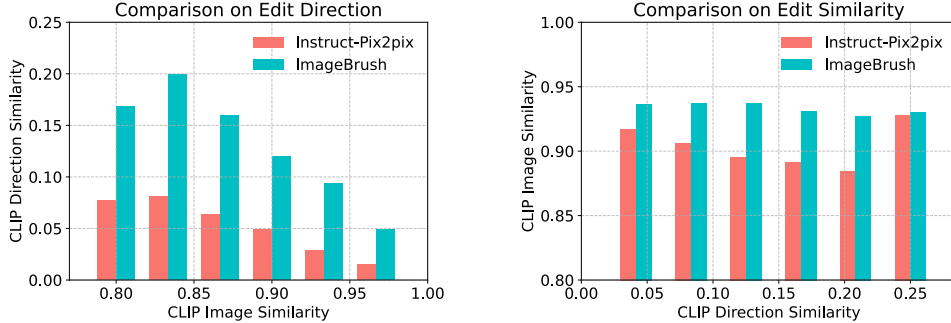


Figure 3: **Quantitative Comparison on Image Editing.** We compare our approach with the representative text-instruction method in terms of direction consistency and similarity consistency.

we employ the Fréchet Inception Score (**FID**) [18] as an evaluation metric. The FID score allows us to evaluate the dissimilarity between the distributions of synthesized images and real images.

Image Generation Paradigm. In the image manipulation task, a pair of transformed images is utilized as visual instructions to edit a target image within the same instruction context. For other tasks, we conduct experiments in a cross-frame prediction setting, where we select two temporally close frames and use one of them as an example to predict the other. Specifically, we employ one frame along with its corresponding label (e.g., edge, semantic segmentation, keypoints, or masked image) as a contextual example, and take the label from another frame as a query to recover that frame. To obtain the label information, we extract keypoints from the UBC-Fashion dataset using OpenPose [8], and for the LRW dataset, we utilize a face parsing network [68] to generate segmentation labels. To ensure that the selected frames belong to the same context, we restrict the optical flow between them to a specific range, maintaining consistency for both training and testing. It is important to note that, for fair comparison, we always utilize the first frame of each video as a reference during the evaluation of the video inpainting task.

Evaluation Results. The comparison results for image manipulation are presented in Fig. 3. We observe that our results exhibit higher image consistency for the same directional similarity values and higher directional similarity values for the same image similarity value. One possible reason is the ability of visual instructions to express certain concepts without a modality gap, which allows our method to better align the edited images.

To demonstrate the versatility of our model, we conducted experiments using in-the-wild videos that encompassed diverse real-world contexts. The results for various downstream tasks are presented in Table 1, showing the superior performance of our approach across all datasets. It is noteworthy that our model achieves these results using a single model, distinguishing it from other methods that require task-specific networks.

4.3 Qualitative Evaluation

We provide a qualitative comparison with SDEdit [33] and Instruct-Pix2pix [6] in Figure 4. In the case of the SDEdit model, we attempted to input both the edit instruction and the output caption, referred to as SDEdit-E and SDEdit-OC, respectively. In contrast to language-guided approaches, our method demonstrates superior fidelity to the provided examples, particularly in capturing text-ambiguous concepts such as holistic style, editing extent, and intricate local object details.

Additionally, we provide a qualitative analysis on a real-world dataset in Figure 5. Compared to CocosNet [72], our approach demonstrates superior visual quality in preserving object structures, as seen in the cabinet and table. It also exhibits higher consistency with the reference appearance, particularly noticeable in the woman’s hair and dress. Furthermore, our method achieves improved shape consistency with the query image, as observed in the mouth. When compared to TSAM [74], our approach yields superior results with enhanced clarity in object shapes and more realistic background filling. These improvements are achieved by effectively leveraging visual cues from the examples.

4.4 Further Analysis

Novel Evaluation Metric. Exemplar-based image manipulation is a novel task, and the evaluation metric in the literature is not suitable for this task. Therefore, we present an evaluation metric

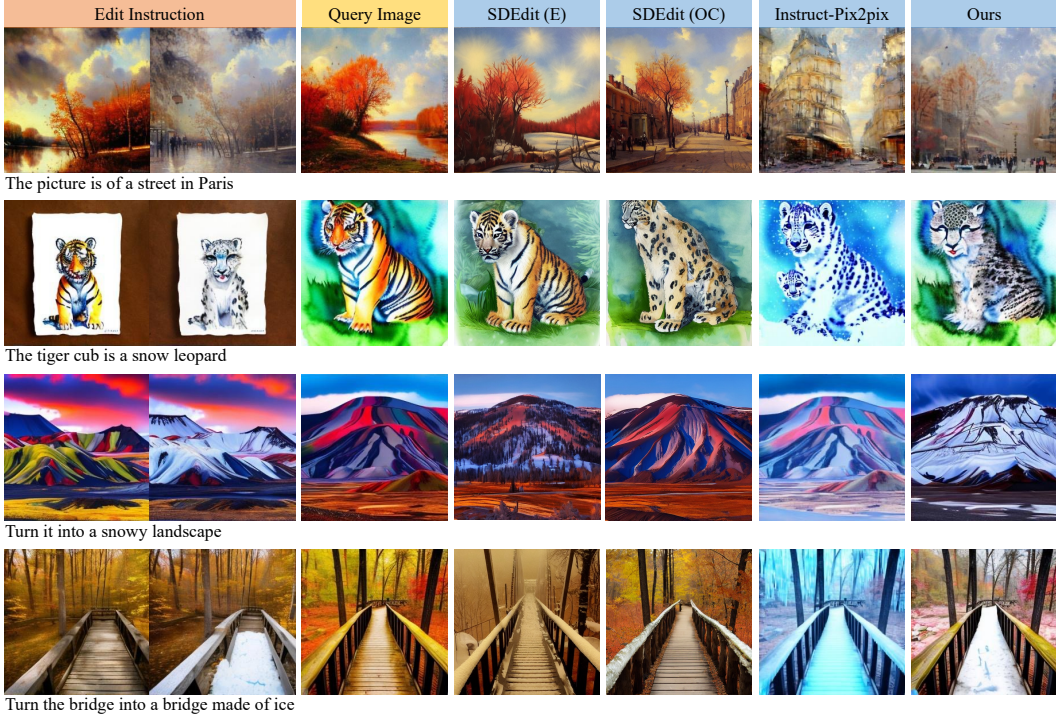


Figure 4: **Qualitative Comparison on Image Manipulation.** In contrast to language-guided approaches, our editing results guided by visual instruction exhibit better compliance with the provided examples.

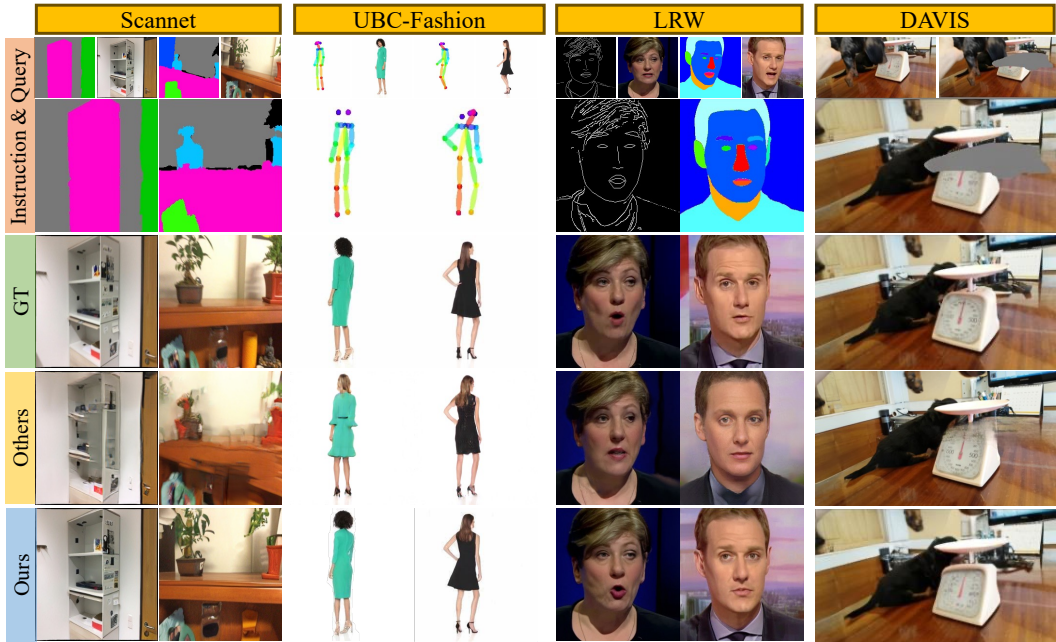


Figure 5: **Qualitative Comparison on In-the-wild Dataset.** We conduct experiments on various downstream tasks including exemplar-based image translation, pose transfer and inpainting.

that requires neither ground-truth image nor human evaluation. Specifically, our model, denoted as Φ_θ , takes the examples $\{\mathbf{E}, \mathbf{E}'\}$, and the source image \mathbf{I} to produce a manipulated output \mathbf{I}' . This procedure is presented as $\mathbf{I}' = \Phi_\theta(\mathbf{I}|\mathbf{E}' \rightarrow \mathbf{E})$. The goal is to let the output image \mathbf{I}' abide by instruction induced from examples \mathbf{E} and \mathbf{E}' while preserving the instruction-invariant content of input image \mathbf{I} . We define prompt fidelity to assess the model’s ability to follow the instruction.



Figure 6: Case Study in Terms of Prompt Fidelity and Image Fidelity.

Table 2: Ablation Study on Image Manipulation. Here we evaluate on our proposed metric.

	w/o Diffusion	w/o Cross-Attention	w/o Interest Region	Full Model
Prompt Fidelity	78.65	39.44	24.29	23.97
Image Fidelity	82.33	41.51	25.74	24.43

According to the symmetry of $\{\mathbf{E}, \mathbf{E}'\}$ and $\{\mathbf{I}, \mathbf{I}'\}$, if its operation strictly follows the instruction, the model should manipulate \mathbf{E} to \mathbf{E}' by using $\mathbf{I} \rightarrow \mathbf{I}'$ as the prompt (see pictures labeled with a dashed yellow tag in Fig. 6). We express the prompt fidelity as follows

$$\Delta_{\text{prompt}} = \text{FID}(\mathbf{E}', \Phi_{\theta}(\mathbf{E}|\mathbf{I} \rightarrow \mathbf{I}')). \quad (8)$$

On the other hand, to evaluate the extent to which the model preserves its content, we introduce an image fidelity metric. If \mathbf{I}' maintains the content of \mathbf{I} , the manipulation should be invertible. That is to say, by using $\mathbf{E}' \rightarrow \mathbf{E}$ as the prompt, the model should reconstruct \mathbf{I} from \mathbf{I}' (see pictures labeled with a dashed blue tag in Fig. 6). Therefore, we define the image fidelity as

$$\Delta_{\text{image}} = \text{FID}(\mathbf{I}, \Phi_{\theta}(\mathbf{I}'|\mathbf{E}' \rightarrow \mathbf{E})). \quad (9)$$

Ablation Study. We performed ablation studies on three crucial components of our method, namely the diffusion process for context exploitation, the vision prompt design, and the injection of human-interest area. Specifically, we conducted experiments on our model by (1) replacing the diffusion process with masked image modeling, (2) removing the cross-attention feature injection obtained from vision prompt module, and (3) deactivating the input of the human interest region. Specifically, we implemented the masked image modeling using the MAE-VQGAN architecture following the best setting of [4]. The numerical results on image manipulation task are shown in Table 2. The results demonstrate the importance of the diffusion process. Without it, the model is unable to progressively comprehend the visual instruction and refine its synthesis, resulting in inferior generation results. When we exclude the feature integration from the visual prompt module, the model struggles to understand high-level semantics, leading to trivial generation results on these instructions. Furthermore, removing the region of interest interface results in a slight decrease in performance, highlighting its effectiveness in capturing human intent.

Case Study. In Figure 6, we present two cases that showcase our model’s performance in terms of image and prompt fidelity. The first case, depicted on the left, highlights our model’s capability to utilize its predicted result \mathbf{I}' to reconstruct \mathbf{I} by transforming the image back to a dark appearance. With predicted \mathbf{I}' , our model also successfully edits the corresponding example from \mathbf{E} to \mathbf{E}' , making the example image colorful. On the right side of the figure, we present a case where our model encounters difficulty in capturing the change in the background, specifically the disappearance of the holographic element.

5 Conclusion

In this article, we present an innovative way of interacting with images, *Image Manipulation by Visual Instruction*. Within this paradigm, we propose a framework, **ImageBrush**, and incorporate carefully designed visual prompt strategy. Through extensive experimentation, we demonstrate the

effectiveness of our visual instruction-driven approach in various image editing tasks and real-world scenarios.

Limitation and Future Work. 1) The proposed model may face challenges when there is a substantial disparity between the given instruction and the query image. 2) The current model also encounters difficulties in handling intricate details, such as subtle background changes or adding small objects. 3) Future work can delve into a broader range of datasets and tasks, paving the way for future generative visual foundation models.

Ethical Consideration. Like all the image generation models, our model can potentially be exploited for malicious purposes such as the synthesis of deceptive or harmful content. We are committed to limiting the use of our model strictly to research purposes.

References

- [1] Yuval Alaluf, Or Patashnik, and Daniel Cohen-Or. Restyle: A residual-based stylegan encoder via iterative refinement. In *Proceedings of the IEEE/CVF International Conference on Computer Vision (ICCV)*, October 2021.
- [2] Omri Avrahami, Ohad Fried, and Dani Lischinski. Blended latent diffusion. *arXiv preprint arXiv:2206.02779*, 2022.
- [3] Aayush Bansal, Yaser Sheikh, and Deva Ramanan. Shapes and context: In-the-wild image synthesis & manipulation. In *Proceedings of the IEEE/CVF Conference on Computer Vision and Pattern Recognition*, pp. 2317–2326, 2019.
- [4] Amir Bar, Yossi Gandelsman, Trevor Darrell, Amir Globerson, and Alexei Efros. Visual prompting via image inpainting. In S. Koyejo, S. Mohamed, A. Agarwal, D. Belgrave, K. Cho, and A. Oh (eds.), *Advances in Neural Information Processing Systems*, volume 35, pp. 25005–25017. Curran Associates, Inc., 2022. URL https://proceedings.neurips.cc/paper_files/paper/2022/file/9f09f316a3eaf59d9ced5ffaefe97e0f-Paper-Conference.pdf.
- [5] Omer Bar-Tal, Dolev Ofri-Amar, Rafail Fridman, Yoni Kasten, and Tali Dekel. Text2live: Text-driven layered image and video editing. In *Computer Vision—ECCV 2022: 17th European Conference, Tel Aviv, Israel, October 23–27, 2022, Proceedings, Part XV*, pp. 707–723. Springer, 2022.
- [6] Tim Brooks, Aleksander Holynski, and Alexei A Efros. Instructpix2pix: Learning to follow image editing instructions. *Proceedings of the IEEE/CVF Conference on Computer Vision and Pattern Recognition*, 2023.
- [7] Tom Brown, Benjamin Mann, Nick Ryder, Melanie Subbiah, Jared D Kaplan, Prafulla Dhariwal, Arvind Neelakantan, Pranav Shyam, Girish Sastry, Amanda Askell, et al. Language models are few-shot learners. *Advances in neural information processing systems*, 33:1877–1901, 2020.
- [8] Zhe Cao, Tomas Simon, Shih-En Wei, and Yaser Sheikh. Realtime multi-person 2d pose estimation using part affinity fields. In *Proceedings of the IEEE conference on computer vision and pattern recognition*, pp. 7291–7299, 2017.
- [9] Huiwen Chang, Han Zhang, Lu Jiang, Ce Liu, and William T Freeman. Maskgit: Masked generative image transformer. In *Proceedings of the IEEE/CVF Conference on Computer Vision and Pattern Recognition*, pp. 11315–11325, 2022.
- [10] J. S. Chung and A. Zisserman. Lip reading in the wild. In *Asian Conference on Computer Vision*, 2016.
- [11] Guillaume Couairon, Jakob Verbeek, Holger Schwenk, and Matthieu Cord. Diffedit: Diffusion-based semantic image editing with mask guidance. *arXiv preprint arXiv:2210.11427*, 2022.
- [12] Angela Dai, Angel X. Chang, Manolis Savva, Maciej Halber, Thomas Funkhouser, and Matthias Nießner. Scannet: Richly-annotated 3d reconstructions of indoor scenes. In *Proc. Computer Vision and Pattern Recognition (CVPR), IEEE*, 2017.
- [13] Yuxin Fang, Quan Sun, Xinggang Wang, Tiejun Huang, Xinlong Wang, and Yue Cao. Eva-02: A visual representation for neon genesis. *arXiv preprint arXiv:2303.11331*, 2023.
- [14] Rinon Gal, Yuval Alaluf, Yuval Atzmon, Or Patashnik, Amit H. Bermano, Gal Chechik, and Daniel Cohen-Or. An image is worth one word: Personalizing text-to-image generation using textual inversion, 2022. URL <https://arxiv.org/abs/2208.01618>.

- [15] Kaiming He, Xinlei Chen, Saining Xie, Yanghao Li, Piotr Dollár, and Ross Girshick. Masked autoencoders are scalable vision learners. In *Proceedings of the IEEE/CVF Conference on Computer Vision and Pattern Recognition (CVPR)*, pp. 16000–16009, June 2022.
- [16] Amir Hertz, Ron Mokady, Jay Tenenbaum, Kfir Aberman, Yael Pritch, and Daniel Cohen-Or. Prompt-to-prompt image editing with cross attention control. *arXiv preprint arXiv:2208.01626*, 2022.
- [17] Aaron Hertzmann, Charles E Jacobs, Nuria Oliver, Brian Curless, and David H Salesin. Image analogies. In *Proceedings of the 28th annual conference on Computer graphics and interactive techniques*, pp. 327–340, 2001.
- [18] Martin Heusel, Hubert Ramsauer, Thomas Unterthiner, Bernhard Nessler, and Sepp Hochreiter. Gans trained by a two time-scale update rule converge to a local nash equilibrium. In I. Guyon, U. Von Luxburg, S. Bengio, H. Wallach, R. Fergus, S. Vishwanathan, and R. Garnett (eds.), *Advances in Neural Information Processing Systems*, volume 30. Curran Associates, Inc., 2017. URL https://proceedings.neurips.cc/paper_files/paper/2017/file/8a1d694707eb0fefe65871369074926d-Paper.pdf.
- [19] Jonathan Ho, Ajay Jain, and Pieter Abbeel. Denoising diffusion probabilistic models. *Advances in Neural Information Processing Systems*, 33:6840–6851, 2020.
- [20] Jonathan Ho, Chitwan Saharia, William Chan, David J. Fleet, Mohammad Norouzi, and Tim Salimans. Cascaded diffusion models for high fidelity image generation. *Journal of Machine Learning Research*, 23(47):1–33, 2022. URL <http://jmlr.org/papers/v23/21-0635.html>.
- [21] Lianghua Huang, Di Chen, Yu Liu, Shen Yujun, Deli Zhao, and Zhou Jingren. Composer: Creative and controllable image synthesis with composable conditions. 2023.
- [22] Xun Huang, Ming-Yu Liu, Serge Belongie, and Jan Kautz. Multimodal unsupervised image-to-image translation. In *Proceedings of the European Conference on Computer Vision (ECCV)*, September 2018.
- [23] P. Isola, J. Zhu, T. Zhou, and A. A. Efros. Image-to-image translation with conditional adversarial networks. In *2017 IEEE Conference on Computer Vision and Pattern Recognition (CVPR)*, pp. 5967–5976, Los Alamitos, CA, USA, jul 2017. IEEE Computer Society. doi: 10.1109/CVPR.2017.632. URL <https://doi.ieeecomputersociety.org/10.1109/CVPR.2017.632>.
- [24] Bahjat Kawar, Shiran Zada, Oran Lang, Omer Tov, Huiwen Chang, Tali Dekel, Inbar Mosseri, and Michal Irani. Imagic: Text-based real image editing with diffusion models. *arXiv preprint arXiv:2210.09276*, 2022.
- [25] Gwanghyun Kim, Taesung Kwon, and Jong Chul Ye. Diffusionclip: Text-guided diffusion models for robust image manipulation. In *Proceedings of the IEEE/CVF Conference on Computer Vision and Pattern Recognition*, pp. 2426–2435, 2022.
- [26] Diederik P. Kingma and Jimmy Ba. Adam: A method for stochastic optimization. *CoRR*, abs/1412.6980, 2014.
- [27] Alexander Kirillov, Eric Mintun, Nikhila Ravi, Hanzi Mao, Chloe Rolland, Laura Gustafson, Tete Xiao, Spencer Whitehead, Alexander C. Berg, Wan-Yen Lo, Piotr Dollár, and Ross Girshick. Segment anything. *arXiv:2304.02643*, 2023.
- [28] Gihyun Kwon and Jong Chul Ye. Diffusion-based image translation using disentangled style and content representation. *arXiv preprint arXiv:2209.15264*, 2022.
- [29] Yuheng Li, Haotian Liu, Qingyang Wu, Fangzhou Mu, Jianwei Yang, Jianfeng Gao, Chunyuan Li, and Yong Jae Lee. Gligen: Open-set grounded text-to-image generation. *CVPR*, 2023.
- [30] Ming-Yu Liu, Thomas Breuel, and Jan Kautz. Unsupervised image-to-image translation networks. In I. Guyon, U. Von Luxburg, S. Bengio, H. Wallach, R. Fergus, S. Vishwanathan, and R. Garnett (eds.), *Advances in Neural Information Processing Systems*, volume 30. Curran Associates, Inc., 2017. URL https://proceedings.neurips.cc/paper_files/paper/2017/file/dc6a6489640ca02b0d42dabeb8e46bb7-Paper.pdf.
- [31] Shilong Liu, Zhaoyang Zeng, Tianhe Ren, Feng Li, Hao Zhang, Jie Yang, Chunyuan Li, Jianwei Yang, Hang Su, Jun Zhu, et al. Grounding dino: Marrying dino with grounded pre-training for open-set object detection. *arXiv preprint arXiv:2303.05499*, 2023.
- [32] Yiyang Ma, Huan Yang, Wenjing Wang, Jianlong Fu, and Jiaying Liu. Unified multi-modal latent diffusion for joint subject and text conditional image generation. *arXiv preprint arXiv:2303.09319*, 2023.

- [33] Chenlin Meng, Yutong He, Yang Song, Jiaming Song, Jiajun Wu, Jun-Yan Zhu, and Stefano Ermon. SDEdit: Guided image synthesis and editing with stochastic differential equations. In *International Conference on Learning Representations*, 2022.
- [34] Ben Mildenhall, Pratul P Srinivasan, Matthew Tancik, Jonathan T Barron, Ravi Ramamoorthi, and Ren Ng. Nerf: Representing scenes as neural radiance fields for view synthesis. *Communications of the ACM*, 65(1):99–106, 2021.
- [35] Ron Mokady, Amir Hertz, Kfir Aberman, Yael Pritch, and Daniel Cohen-Or. Null-text inversion for editing real images using guided diffusion models. *arXiv preprint arXiv:2211.09794*, 2022.
- [36] Chong Mou, Xintao Wang, Liangbin Xie, Jian Zhang, Zhongang Qi, Ying Shan, and Xiaohu Qie. T2i-adapter: Learning adapters to dig out more controllable ability for text-to-image diffusion models. *arXiv preprint arXiv:2302.08453*, 2023.
- [37] Alex Nichol, Prafulla Dhariwal, Aditya Ramesh, Pranav Shyam, Pamela Mishkin, Bob McGrew, Ilya Sutskever, and Mark Chen. Glide: Towards photorealistic image generation and editing with text-guided diffusion models. *arXiv preprint arXiv:2112.10741*, 2021.
- [38] Long Ouyang, Jeffrey Wu, Xu Jiang, Diogo Almeida, Carroll Wainwright, Pamela Mishkin, Chong Zhang, Sandhini Agarwal, Katarina Slama, Alex Ray, John Schulman, Jacob Hilton, Fraser Kelton, Luke Miller, Maddie Simens, Amanda Askell, Peter Welinder, Paul F Christiano, Jan Leike, and Ryan Lowe. Training language models to follow instructions with human feedback. In S. Koyejo, S. Mohamed, A. Agarwal, D. Belgrave, K. Cho, and A. Oh (eds.), *Advances in Neural Information Processing Systems*, volume 35, pp. 27730–27744. Curran Associates, Inc., 2022. URL https://proceedings.neurips.cc/paper_files/paper/2022/file/b1efde53be364a73914f58805a001731-Paper-Conference.pdf.
- [39] Taesung Park, Ming-Yu Liu, Ting-Chun Wang, and Jun-Yan Zhu. Semantic image synthesis with spatially-adaptive normalization. In *Proceedings of the IEEE/CVF Conference on Computer Vision and Pattern Recognition (CVPR)*, June 2019.
- [40] Adam Paszke, Sam Gross, Francisco Massa, Adam Lerer, James Bradbury, Gregory Chanan, Trevor Killeen, Zeming Lin, Natalia Gimelshein, Luca Antiga, Alban Desmaison, Andreas Köpf, Edward Yang, Zach DeVito, Martin Raison, Alykhan Tejani, Sasank Chilamkurthy, Benoit Steiner, Lu Fang, Junjie Bai, and Soumith Chintala. Pytorch: An imperative style, high-performance deep learning library. *Proceedings of the 33rd International Conference on Neural Information Processing Systems*, 2019.
- [41] Baolin Peng, Chunyuan Li, Pengcheng He, Michel Galley, and Jianfeng Gao. Instruction tuning with gpt-4. *arXiv preprint arXiv:2304.03277*, 2023.
- [42] F. Perazzi, J. Pont-Tuset, B. McWilliams, L. Van Gool, M. Gross, and A. Sorkine-Hornung. A benchmark dataset and evaluation methodology for video object segmentation. In *Computer Vision and Pattern Recognition*, 2016.
- [43] Xiaojuan Qi, Qifeng Chen, Jiaya Jia, and Vladlen Koltun. Semi-parametric image synthesis. In *Proceedings of the IEEE Conference on Computer Vision and Pattern Recognition (CVPR)*, June 2018.
- [44] Lawrence R Rabiner. A tutorial on hidden markov models and selected applications in speech recognition. *Proceedings of the IEEE*, 77(2):257–286, 1989.
- [45] Alec Radford, Jong Wook Kim, Chris Hallacy, Aditya Ramesh, Gabriel Goh, Sandhini Agarwal, Girish Sastry, Amanda Askell, Pamela Mishkin, Jack Clark, et al. Learning transferable visual models from natural language supervision. In *International conference on machine learning*, pp. 8748–8763. PMLR, 2021.
- [46] Aditya Ramesh, Prafulla Dhariwal, Alex Nichol, Casey Chu, and Mark Chen. Hierarchical text-conditional image generation with clip latents. *arXiv preprint arXiv:2204.06125*, 2022.
- [47] Elad Richardson, Yuval Alaluf, Or Patashnik, Yotam Nitzan, Yaniv Azar, Stav Shapiro, and Daniel Cohen-Or. Encoding in style: A stylegan encoder for image-to-image translation. In *Proceedings of the IEEE/CVF Conference on Computer Vision and Pattern Recognition (CVPR)*, pp. 2287–2296, June 2021.
- [48] Robin Rombach, Andreas Blattmann, Dominik Lorenz, Patrick Esser, and Björn Ommer. High-resolution image synthesis with latent diffusion models. In *Proceedings of the IEEE/CVF Conference on Computer Vision and Pattern Recognition*, pp. 10684–10695, 2022.
- [49] Nataniel Ruiz, Yuanzhen Li, Varun Jampani, Yael Pritch, Michael Rubinstein, and Kfir Aberman. Dreambooth: Fine tuning text-to-image diffusion models for subject-driven generation. In *Proceedings of the IEEE/CVF Conference on Computer Vision and Pattern Recognition*, 2023.

- [50] Chitwan Saharia, William Chan, Huiwen Chang, Chris Lee, Jonathan Ho, Tim Salimans, David Fleet, and Mohammad Norouzi. Palette: Image-to-image diffusion models. In *ACM SIGGRAPH 2022 Conference Proceedings*, SIGGRAPH '22, New York, NY, USA, 2022. Association for Computing Machinery. ISBN 9781450393379. doi: 10.1145/3528233.3530757. URL <https://doi.org/10.1145/3528233.3530757>.
- [51] Chitwan Saharia, William Chan, Saurabh Saxena, Lala Li, Jay Whang, Emily L Denton, Kamyar Ghasemipour, Raphael Gontijo Lopes, Burcu Karagol Ayan, Tim Salimans, et al. Photorealistic text-to-image diffusion models with deep language understanding. *Advances in Neural Information Processing Systems*, 35:36479–36494, 2022.
- [52] Aleksandar Shtedritski, Christian Rupprecht, and Andrea Vedaldi. What does clip know about a red circle? visual prompt engineering for vlms. *arXiv preprint arXiv:2304.06712*, 2023.
- [53] Jiaming Song, Chenlin Meng, and Stefano Ermon. Denoising diffusion implicit models. *arXiv preprint arXiv:2010.02502*, 2020.
- [54] Yang Song and Stefano Ermon. Generative modeling by estimating gradients of the data distribution. *Advances in neural information processing systems*, 32, 2019.
- [55] Omer Tov, Yuval Alaluf, Yotam Nitzan, Or Patashnik, and Daniel Cohen-Or. Designing an encoder for stylegan image manipulation. *ACM Trans. Graph.*, 40(4), jul 2021. ISSN 0730-0301. doi: 10.1145/3450626.3459838. URL <https://doi.org/10.1145/3450626.3459838>.
- [56] Narek Tumanyan, Omer Bar-Tal, Shai Bagon, and Tali Dekel. Splicing vit features for semantic appearance transfer. In *Proceedings of the IEEE/CVF Conference on Computer Vision and Pattern Recognition*, pp. 10748–10757, 2022.
- [57] Narek Tumanyan, Michal Geyer, Shai Bagon, and Tali Dekel. Plug-and-play diffusion features for text-driven image-to-image translation. *Proceedings of the IEEE/CVF Conference on Computer Vision and Pattern Recognition*, 2023.
- [58] Dani Valevski, Matan Kalman, Yossi Matias, and Yaniv Leviathan. Unitune: Text-driven image editing by fine tuning an image generation model on a single image. *arXiv preprint arXiv:2210.09477*, 2022.
- [59] Yael Vinker, Eliahu Horwitz, Nir Zabari, and Yedid Hoshen. Image shape manipulation from a single augmented training sample. In *Proceedings of the IEEE/CVF International Conference on Computer Vision*, pp. 13769–13778, 2021.
- [60] Andrey Voynov, Qinghao Chu, Daniel Cohen-Or, and Kfir Aberman. $p+$: Extended textual conditioning in text-to-image generation. *arXiv preprint arXiv:2303.09522*, 2023.
- [61] Miao Wang, Guo-Ye Yang, Ruilong Li, Run-Ze Liang, Song-Hai Zhang, Peter M Hall, and Shi-Min Hu. Example-guided style-consistent image synthesis from semantic labeling. In *Proceedings of the IEEE/CVF conference on computer vision and pattern recognition*, pp. 1495–1504, 2019.
- [62] Ting-Chun Wang, Ming-Yu Liu, Jun-Yan Zhu, Andrew Tao, Jan Kautz, and Bryan Catanzaro. High-resolution image synthesis and semantic manipulation with conditional gans. *2018 IEEE/CVF Conference on Computer Vision and Pattern Recognition*, pp. 8798–8807, 2017.
- [63] Xinlong Wang, Wen Wang, Yue Cao, Chunhua Shen, and Tiejun Huang. Images speak in images: A generalist painter for in-context visual learning. *Proceedings of the IEEE/CVF Conference on Computer Vision and Pattern Recognition*, 2023.
- [64] Yuxin Wen, Neel Jain, John Kirchenbauer, Micah Goldblum, Jonas Geiping, and Tom Goldstein. Hard prompts made easy: Gradient-based discrete optimization for prompt tuning and discovery. *arXiv preprint arXiv:2302.03668*, 2023.
- [65] Xingqian Xu, Zhangyang Wang, Eric Zhang, Kai Wang, and Humphrey Shi. Versatile diffusion: Text, images and variations all in one diffusion model. 2022. URL <https://arxiv.org/abs/2211.08332>.
- [66] Binxin Yang, Shuyang Gu, Bo Zhang, Ting Zhang, Xuejin Chen, Xiaoyan Sun, Dong Chen, and Fang Wen. Paint by example: Exemplar-based image editing with diffusion models. *arXiv preprint arXiv:2211.13227*, 2022.
- [67] Zili Yi, Hao Zhang, Ping Tan, and Minglun Gong. Dualgan: Unsupervised dual learning for image-to-image translation. In *2017 IEEE International Conference on Computer Vision (ICCV)*, pp. 2868–2876, 2017. doi: 10.1109/ICCV.2017.310.

- [68] Changqian Yu, Changxin Gao, Jingbo Wang, Gang Yu, Chunhua Shen, and Nong Sang. Bisenet v2: Bilateral network with guided aggregation for real-time semantic segmentation. *Int. J. Comput. Vision*, 129(11):3051–3068, nov 2021. ISSN 0920-5691. doi: 10.1007/s11263-021-01515-2. URL <https://doi.org/10.1007/s11263-021-01515-2>.
- [69] Polina Zablotskaia, Aliaksandr Siarohin, Bo Zhao, and Leonid Sigal. Dwnet: Dense warp-based network for pose-guided human video generation. In *British Machine Vision Conference*, 2019.
- [70] Bo Zhang, Mingming He, Jing Liao, Pedro V Sander, Lu Yuan, Amine Bermak, and Dong Chen. Deep exemplar-based video colorization. In *Proceedings of the IEEE/CVF conference on computer vision and pattern recognition*, pp. 8052–8061, 2019.
- [71] Lvmin Zhang and Maneesh Agrawala. Adding conditional control to text-to-image diffusion models. *arXiv preprint arXiv:2302.05543*, 2023.
- [72] Pan Zhang, Bo Zhang, Dong Chen, Lu Yuan, and Fang Wen. Cross-domain correspondence learning for exemplar-based image translation. In *Proceedings of the IEEE/CVF Conference on Computer Vision and Pattern Recognition*, pp. 5143–5153, 2020.
- [73] Yuanhan Zhang, Kaiyang Zhou, and Ziwei Liu. What makes good examples for visual in-context learning? *arXiv preprint arXiv:2301.13670*, 2023.
- [74] Xueyan Zou, Linjie Yang, Ding Liu, and Yong Jae Lee. Progressive temporal feature alignment network for video inpainting. In *CVPR*, 2021.

Appendices

A Analysis of In-Context Instruction with Multiple Examples

Our approach can be naturally extended to include multiple examples. Specifically, given a series of examples $\{\mathbf{E}_1, \mathbf{E}'_1, \dots, \mathbf{E}_n, \mathbf{E}'_n, \mathbf{I}\}$, where n represents the number of support examples, our objective is to generate \mathbf{I}' . In our main paper, we primarily focused on the special case where $n = 1$. When dealing with multiple examples, we could also establish their spatial correspondence by directly concatenating them as input to our UNet architecture. Specifically, we create a grid $x_{t-1} = \text{Grid}(\{\mathbf{E}_1, \mathbf{E}'_1, \dots, \mathbf{E}_n, \mathbf{E}'_n, \mathbf{I}\}_{t-1})$ that can accommodate up to eight examples following [4]. To facilitate contextual learning, we extend the input length of our prompt encoder e_p , and incorporate tokenized representations of these collections of examples as input to it. In this way, our framework is able to handle cases that involve multiple examples.

Below we discuss the impact of these examples on our model’s final performance by varying their numbers and orders.

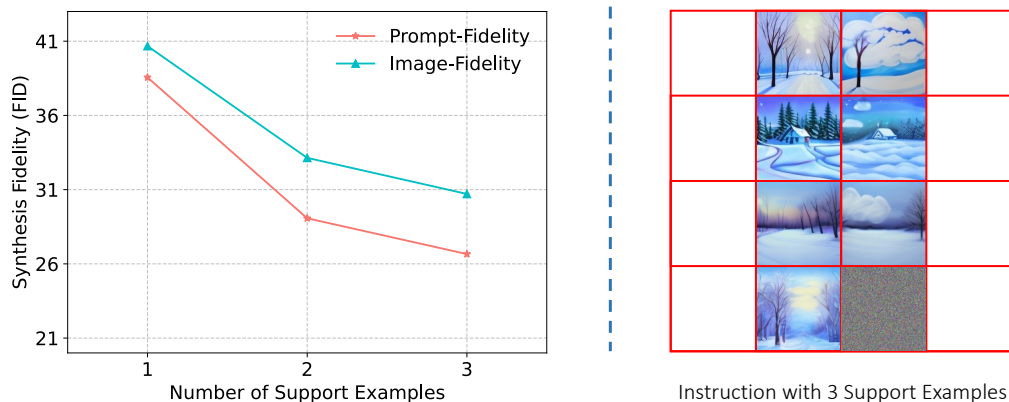


Figure 7: Analysis of In-Context Instruction with Multiple Examples.

A.1 Number of In-Context Examples.

In our dataset, which typically consists of 4 examples, we examine the influence of the number of in-context examples by varying it from 1 to 3, as illustrated in Figure 7. We evaluate this variation using our proposed metrics: prompt fidelity Δ_{prompt} and image fidelity Δ_{image} , which assess instruction adherence and content consistency, respectively. The results demonstrate that increasing the number of support examples enhances performance, potentially by reducing task ambiguity.

Furthermore, we present additional instruction results in Figure 9, showcasing the impact of different numbers of in-context examples. It is clear that as the number of examples increases, the model becomes more confident in comprehending the task description. This is particularly evident in the second row, where the synthesized floor becomes smoother and the rainbow appears more distinct. Similarly, in the third row, the wormhole becomes complete. However, for simpler tasks that can be adequately induced with just one example (as demonstrated in the last row), increasing the number of examples does not lead to further performance improvements.

A.2 Order of In-Context Examples.

We have also conducted an investigation into the impact of the order of support examples by shuffling them. Through empirical analysis, we found no evidence suggesting that the order of the examples has any impact on performance. This finding aligns with our initial expectation, as there is no sequential logic present in our examples.

B Case Study on Visual Prompt User Interface

In our work, we have developed a human interface to further enhance our model’s ability to understand human intent. Since manual labeling of human-intended bounding boxes is not available, we utilize language-grounded boxes [31] to train the network in our experiments. In Figure 8, we demonstrate the difference when the bounding box is utilized during inference. We can observe that when the crown area is further emphasized by bounding box, the synthesized crown exhibits a more consistent style with the provided example. Additionally, the dress before the chest area is better preserved.



Figure 8: **Analysis of Visual Prompt User Interface.** On the left side, we illustrate the usual case, while on the right side, we present a scenario where a bounding box (indicated by the yellow box) is grounded by DINO as the model input.

C More Visual Instruction Results

In this section, we present additional visual instruction results, where the synthesized result is highlighted within the red box. These results demonstrate the effectiveness of our approach in handling diverse manipulation types, including style transfer, object swapping, and composite operations, as showcased in Fig. 10 and Fig. 11. Furthermore, our method demonstrates its versatility across real-world datasets, successfully tackling various downstream tasks, such as image translation, pose translation, and inpainting in Fig. 12 and Fig. 13. Importantly, it is worth noting that all the presented results are generated by a single model.

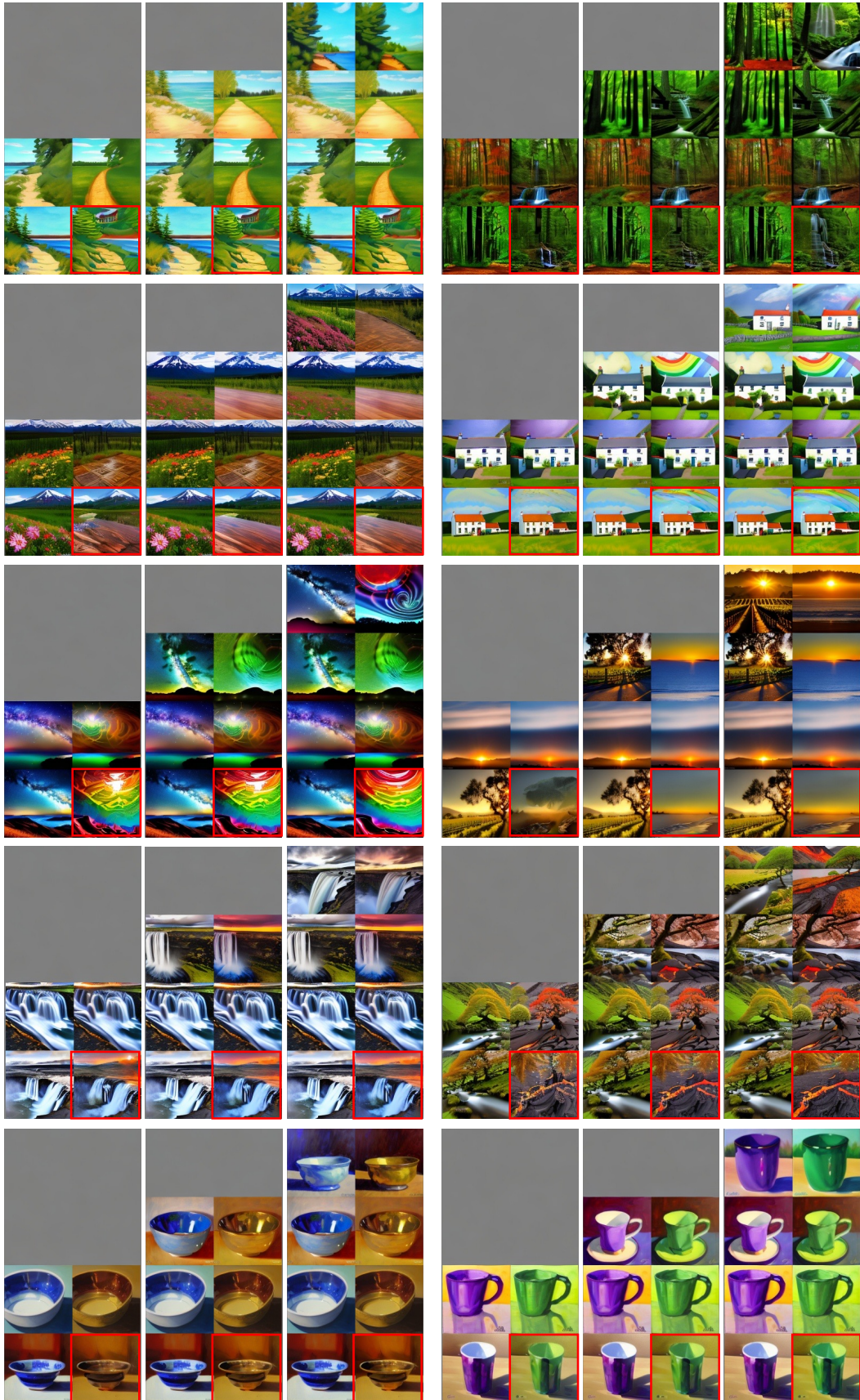


Figure 9: Qualitative Analysis on Number of In-Context Examples.

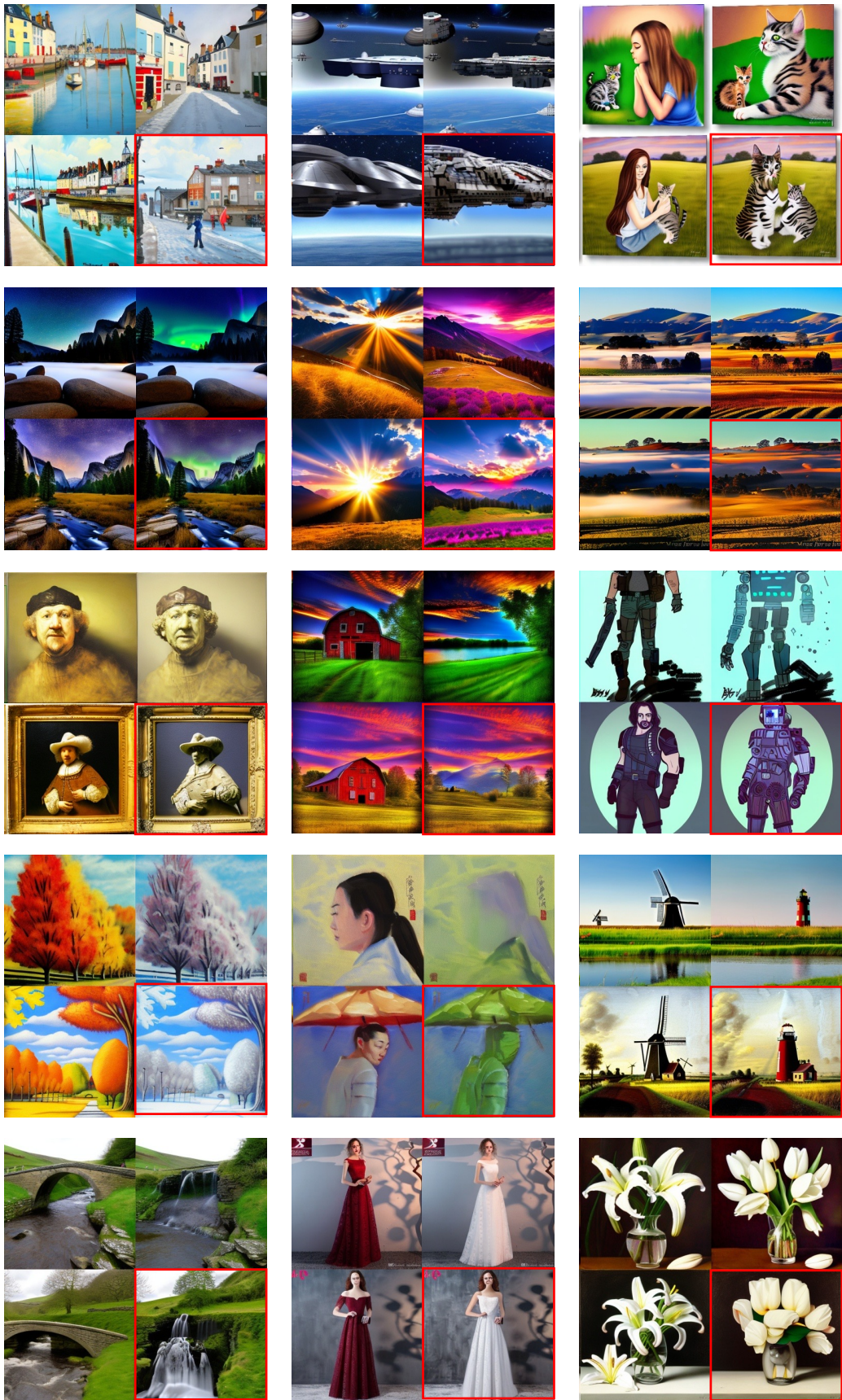


Figure 10: Image Manipulation Results by Visual Instruction.

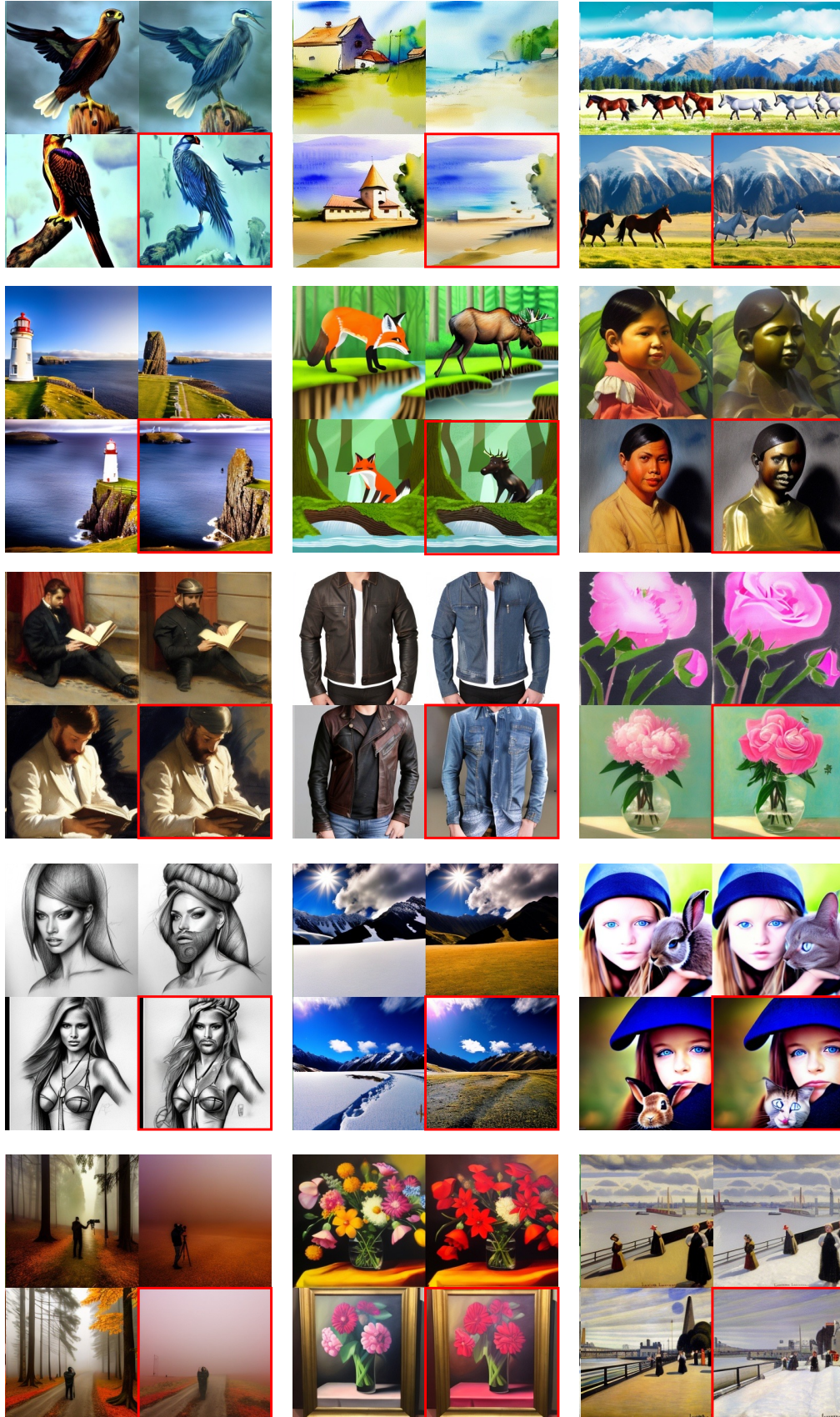


Figure 11: Image Manipulation Results by Visual Instruction.

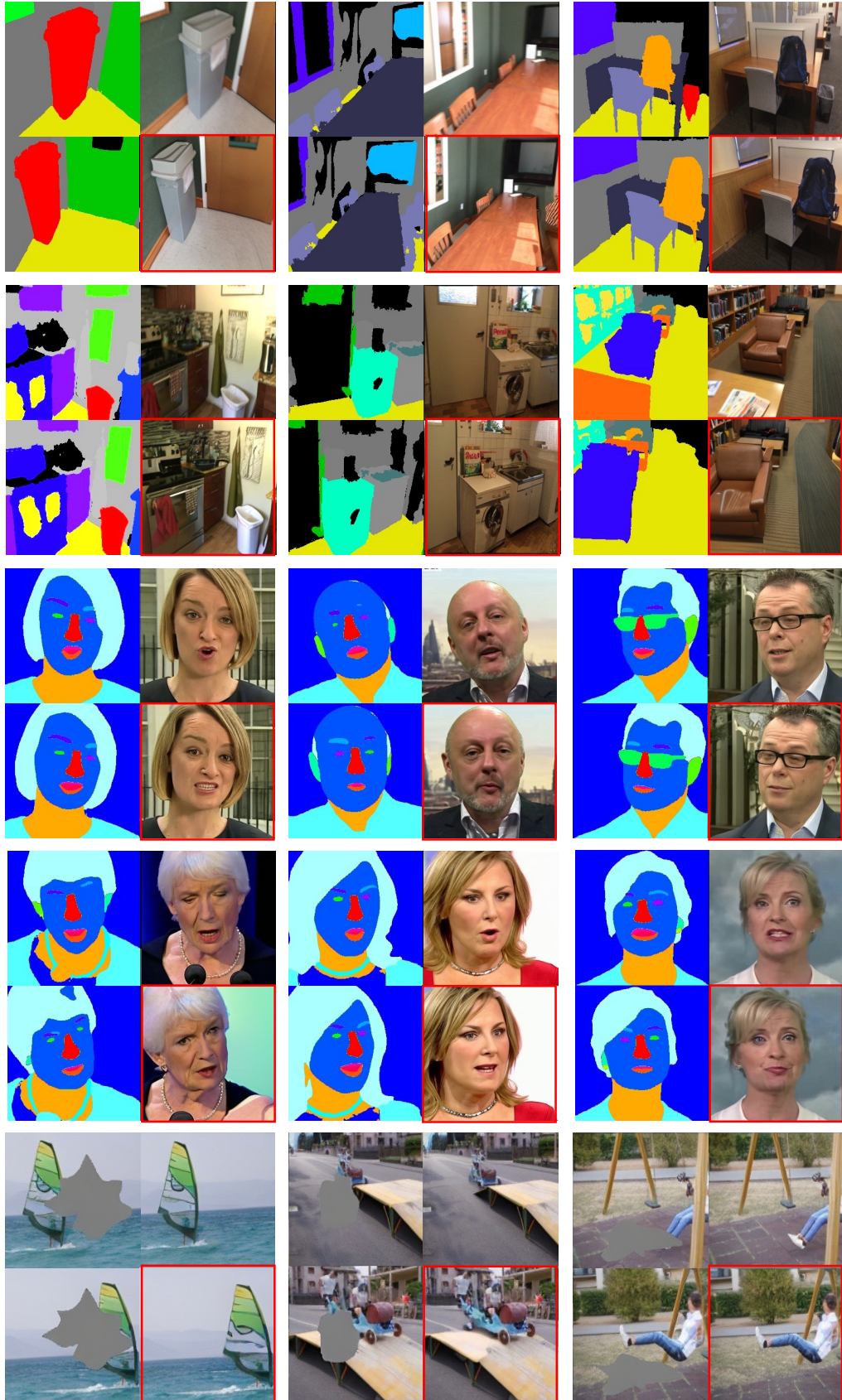


Figure 12: Instruction Results on In-the-wild Dataset.



Figure 13: Instruction Results on In-the-wild Dataset.